The 15th International Symposium on Magnetic Bearings, August 3-6, 2016, Mojiko Hotel, Kitakyushu, Japan

ISMB15

Modeling of a Single Point Suspended Electromagnetic Suspension Carrier System -Study on Rolling Motion-

Shogo HIDA*, Mimpei MORISHITA*

*Graduate School of Electric Engineering and Electronics, Kogakuin University,
2665-1 Nakano-machi Hachioji, 192-0015, Tokyo, Japan

Abstract

Authors made a single point suspended electromagnetic suspension (EMS) system. This EMS system was applied to a transport system. This transport system has a carrier and a guide. The carrier is provided with a magnet unit and a carrier body. The magnet unit which comprises two coils, two iron core and a permanent magnet, suspends the carrier with no contact. The guide comprises an iron plate and propelling coils. When the carrier passes through the curved section of the guide, pendulum motion occurs in the rolling direction. This is rolling motion. The rolling motion continues longer than the pitching motion caused by acceleration and deceleration. When the carrier is swaying, eddy current mainly induces in the iron plate because a magnetic field in an air gap between the iron core and the iron plate changes. The eddy current makes a difference of the convergence times between the rolling and the pitching motions. Our former research modeled the pitching motion of the carrier by considering the eddy current loss and a movement of the action point of the attractive force acting on the magnet unit. In this paper, authors make the model of the rolling motion by the same method. The validity of the modeling method is verified with simulational and experimental results.

Keywords : electromagnetic suspension(EMS), single point suspension, rolling motion, eddy current, damping factor, 3D real time magnetic field solver, electromagnetic field analysis

1. Introduction

Many maglev systems need plural electromagnets to keep the system stability in every component of the motion. Some of them are provided with mechanical suspensions to stabilize each component of the oscillation. Such stabilization leads to structural complexity. They have been a barrier against dissemination of maglev technology. Authors made a single point suspended EMS system to simplify the system structure [1]. In this system, pendulum motion occurs in the rolling direction when the carrier is passes through the curved section. The rolling motion continues longer than the pitching motion caused by acceleration and deceleration. Authors investigated the course of that. As a result, it was clear that the eddy current loss in the iron core and the iron plate makes the convergence time different. Variation of the attractive force and torque influences a period of the pendulum motion [2].

This paper will construct the model of the rolling motion by using the same method as the modeling of the pitching motion and verify the modeling method with the simulational and experimental results.

2. Single point suspended electromagnetic suspension system

The simplified transport system is composed of a carrier with the single point suspended EMS and propelling coils mounted on the under-surface of the iron plate. Figure 1 shows a schematic of the system.

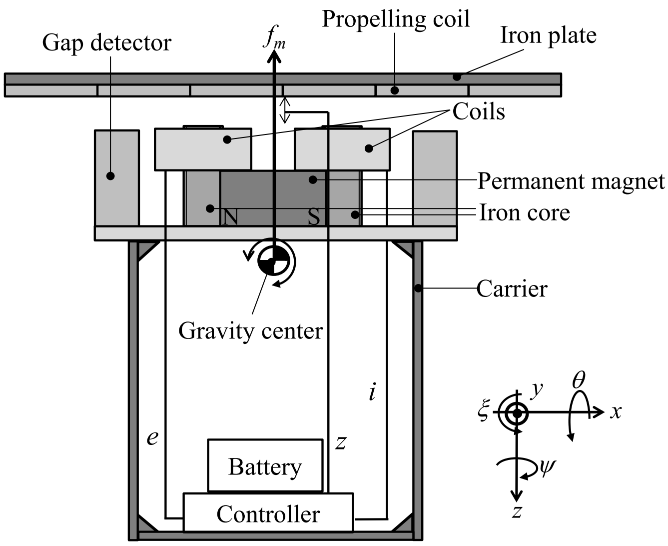

Fig. 1 Outline of equipment

2.1 Carrier structure and levitation control

The carrier comprises a magnet unit and a carrier body, two gap detectors to detect the gap length between the magnet unit and the iron plate. The magnet unit has a permanent magnet and electromagnets. The attractive force acting between the magnet unit and the iron plate is inversely proportional to the square of the gap length. The levitation controller makes the EMS system stable while coil current converges to zero against any stepwise external forces. In other words, the EMS system can be levitated by only permanent magnet attractive force without any coil current. We call such levitation control "Zero-power control" [3].

2.2 Propulsion and guide system

The propulsion and guide system is composed of propelling coils and hall sensors attached on the under surface of the iron plate [4]. The propelling coils are excited on the basis of outputs of the hall sensor as a brushless direct current motor. The traveling magnetic field generated by the propelling coils gives thrust and guide forces to the carrier.

2.3 Basic equation of motion of EMS system

Equation (1) shows the equation of motion and the voltage equation for the single point suspended EMS system [4].

$$
\begin{aligned}
&m\ddot{z} = f_{\mathrm{m}}(z,i) + mg + f_d \\
&I_\theta \ddot{\theta} = f_{\mathrm{m}}(z,i) l_r \sin\theta + T_d \\
&L_0(z)\dot{i} = -N\frac{\partial \Phi(z,i)}{\partial z'}\dot{z} - Ri + e
\end{aligned}
\qquad (1)
$$

Here, z is the air gap length between the iron plate and the magnet unit, i is the excitation current, m is the total mass of the carrier and its load, g is the gravitational acceleration, f_d is the external force, f_m is the magnetically attractive force, I_θ is the total moment of inertia of the carrier, T_d is the external torque, l_r is the length between the carrier gravity center and the top of the magnet unit, θ is the angle of an inclination of the carrier, L_0 is the self-inductance for the coils, N is the number of turns of the coils, Φ is the main flux for the magnetic circuit, R is the coil resistance, e is excitation voltage to the electromagnets, " $\dot{}$ " means time derivative.

3. Analysis of eddy current

When the carrier is swaying, eddy current mainly occurs in the iron plate because a magnetic field in an air gap between the iron core and the iron plate changes. This is one of the causes of the damping factors for the pendulum motion. So, new equation of motion will be had to consider them [2]. The eddy current loss in the iron core and the iron plate is analyzed by using Qm® (3D real time magnetic field solver), to calculate the velocity resistance.

3. 1 Separating of rolling motion

It is necessary to separate the rolling motion into three directions y, z and θ in order to analyze the eddy current loss by using Qm® as shown in Figure 2. These components are the horizontal oscillation expressed by $A_y \sin 2\pi f_p t$, the vertical oscillation expressed by $A_z \sin 4\pi f_p t$, the rotation oscillation expressed by $A_\theta \sin 2\pi f_p t$, respectively. Each amplitude, A_y, A_z or A_θ was calculated with l_r, and θ. Figure 2 shows each direction and amplitude at separating rolling motion. Here, f_p is the rolling frequency.

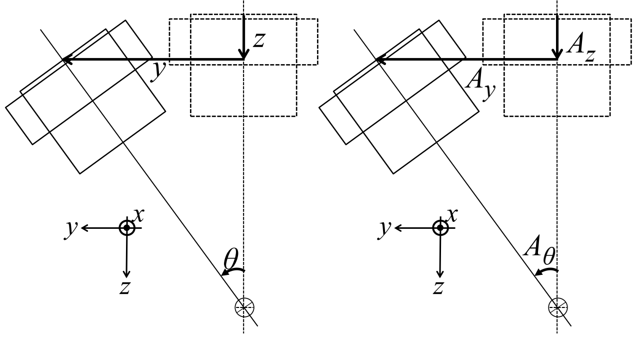

(a) Direction (b) Amplitude

Fig. 2 Separating of rolling motion

3.2 Velocity of each direction oscillation

Equation (2) shows the velocities for the rolling the angular velocity.

$$\begin{aligned} \overline{\omega} &= \sqrt{2} \times A_\theta \times f_p \times \pi \\ \overline{v_y} &= \sqrt{2} \times A_y \times f_p \times \pi \\ \overline{v_z} &= 2\sqrt{2} A_z \times f_p \times \pi \end{aligned} \tag{2}$$

Here, $\overline{v_y}$, $\overline{v_z}$, and $\overline{\omega}$ are the effective values of $\dot{y}$, $\dot{z}$ and $\dot{\omega}$, respectively.

3.3 Calculation of velocity resistance

The velocity resistance, ρ_y, ρ_z, ρ_θ, and $\rho_{\theta ALL}$ are calculated from the analyzed eddy current losses, P_θ, P_y and P_z with Equation (3). Table 1 shows calculation results and the eddy current loss.

$$\begin{aligned} &\rho_y = \frac{P_y}{\overline{v_y}^2}, \rho_z = \frac{P_z}{\overline{v_z}^2}, \rho_\theta = \frac{P_\theta}{\overline{\omega}^2} \\ &\rho_{\theta ALL} = \rho_\theta + l_r \rho_y \cos\theta + l_r \rho_z \sin\theta \end{aligned} \tag{3}$$

Here, P_y is the horizontal eddy current loss, P_z is the vertical eddy current loss, P_θ is the rotation eddy current loss, ρ_y is the horizontal damping factor, ρ_z is the vertical damping factor, ρ_θ is the rotation damping factor, $\rho_{\theta ALL}$ is the damping factor around the center of gravity.

Table 1 Analysis and calculation result of damping factor (lr=0.059[m], θ=5.0[deg], z_0=13[mm])

	θ	y	z	
Velocity root mean square v	0.3877 [rad/s]	23.0 [mm/s]	1.01 [mm/s]	
Eddy current loss P [mW]	0.495	2.010	0.0016	
Velocity resistance ρ	ρ_θ	ρ_y	ρ_z	$\rho_{\theta ALL}$
	7.65 [μN/(rad/s)]	3.806 [mN/(m/s)]	18.97 [mN/(m/s)]	0.332 [mN/(rad/s)]

4. Analysis of attractive force

When the carrier is swaying, the attractive force of magnet unit responds to the air gap between the iron core and iron plate. The attractive force is analyzed by using JMAG® (electromagnetic field analysis software) to calculate variations of attractive force and torque which influence the period of pendulum motion. In this analysis, the air gap, z, changes 9 to 15 [mm]. Inclination of the carrier, θ, also changes 0 to 8 [deg]. Figure 3 shows model of rolling motion.

4.1 Attractive force variation due to inclination

The attractive force fluctuation ratio is obtained by using analysis results, $f_{m\theta}$, f_m and Equation (4). Figure 4 shows the relation between θ and calculation of the attractive force fluctuation ratio, $k(z.\theta)$.

$$h(z',\theta) = \frac{f_{m\theta}}{f_m} \tag{4}$$

Here, f_m is the attractive force without inclination, $f_{m\theta}$ is the attractive force at θ, z' is the air gap considered θ $(z' = z + 2l_r \sin^2(\theta/2))$

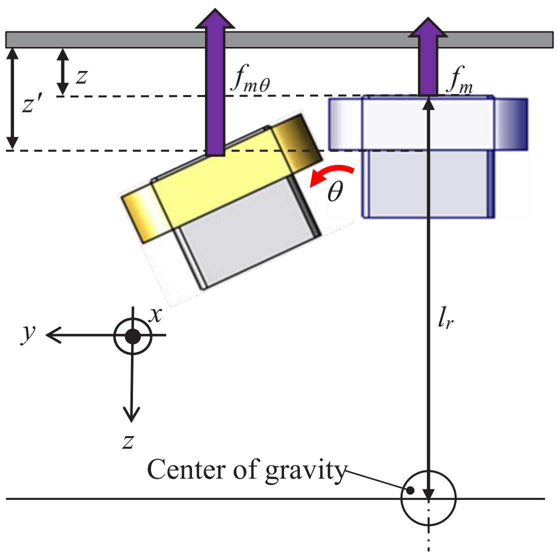

Fig. 3 Model of rolling motion

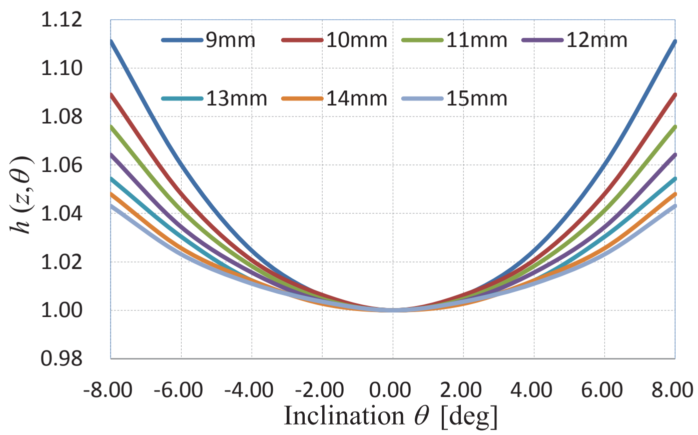

Fig. 4 Calculation result of attractive force fluctuation ratio

4.2 Torque variation due to inclination

Torque is acted on the magnet unit when the carrier as shown Figure 5 is swaying. The torque is calculated by the following expression.

$$\vec{M}_\theta = \vec{l}_r \times \vec{F} \tag{5}$$

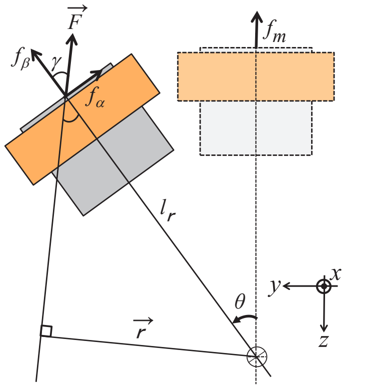

Fig. 5 Torque acting on the carrier

Here, M_θ is the torque acting on carrier. F is the attractive force acting on the center of the top surface of the iron core and "→" denotes a vector. In Figure 5, the following relations are satisfied. Accordingly, Equation (5) can be expressed as follows.

$$\begin{aligned} F &= \frac{f_\alpha}{\sin\gamma} \\ \sin\gamma &= \frac{r}{l_r} \\ r &= l_r \times \sin\gamma \\ \vec{M}_\theta &= l_r f_\alpha + \delta y_G f_\beta \end{aligned} \tag{6}$$

Here, f_α is the horizontal attractive force on the iron core top surface, f_β is the vertical attractive force on the iron core top surface, γ is the angle between $\vec{F}$ and f_β, $\vec{r}$ is a vector for the length between point of action for $\vec{F}$ and the carrier gravity center, δy_G is the action point of f_β.

$$k(z',\theta) = \frac{M_\theta}{f_m} \tag{7}$$

The torque variation ratio due to the inclination is expressed with Equation (7) as the virtual effort distance. Figure 6 shows the relation between θ and the torque variation ratio, $k(z',\theta)$.

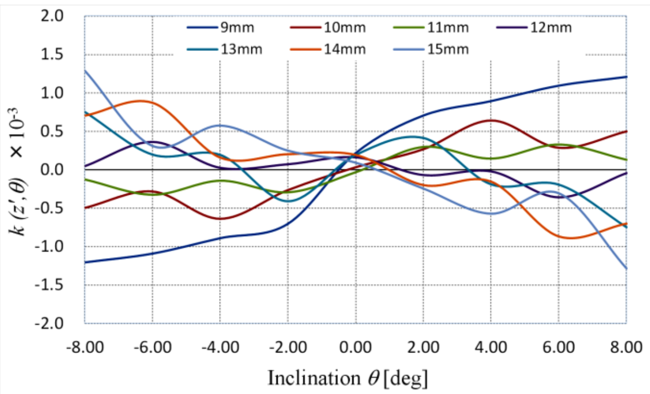

Fig. 6 Torque acting on the carrier

4.3 Movement of action point for attractive force

The torque variation ratio was calculated by using l_r. However the torque variation ratio is influenced by the movement of the action point for the attractive force, δy_G, due to the inclination [2]. The iron cores divided as shown in Figure 7 to calculate the movement of the action point for the attractive force on the iron cores. The length between the carrier gravity center and it can be consider that action point, lr' is expressed with Equation (8). Table 2 shows calculation results of δy_G and lr'.

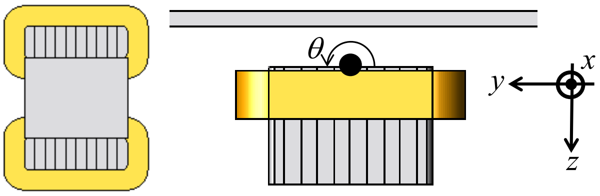

(a) Bottom view (b) Front view

Fig. 7 Divide the iron core

Table 2 Calculation result of the movement of action point for attractive force (lr=59[mm])

θ [deg]	δy_G [mm]	lr' [mm]
0.0	0.000	59.000
1.0	0.551	59.003
2.0	1.111	59.010
3.0	1.695	59.024
4.0	2.315	59.045
5.0	2.881	59.070
6.0	3.489	59.103
7.0	3.940	59.131

$$\varphi = \arctan\left(\frac{\delta y_G}{l_r}\right)$$
$$l_r' = \frac{l_r}{\cos\varphi} \tag{8}$$

Here, ϕ is the angle between l_r and l_r'.

It can be considered that the movement of the action point for the attractive force isn't so important to the torque variation due to inclination.

5. Simulation and experiment

Equation (9) shows the equation of rolling motion, which includes damping factors due to the eddy current loss with the rolling motion. It is the same as the model of the pitching motion.

$$\begin{cases} m\ddot{z} = f_m(z',i)h(z',\theta) + \rho_z \dot{z} + mg + f_d \\ I_\theta \ddot{\theta} = f_m(z',i) l_r \sin\theta + f_m(z',i)k'(z',\theta) + \rho_{\theta ALL}\dot{\theta} + T_d \end{cases} \tag{9}$$

Authors simulated the rolling motion of the carrier to investigate the effectiveness of the damping factor affects to the rolling motion. In this simulation, the carrier was inclined by 5.0 degrees initially and levitated under the zero-power control. Then the carrier was released.

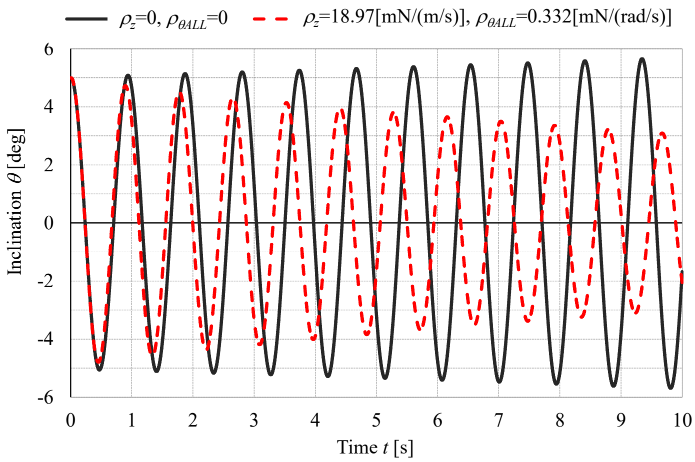

Fig. 8 Simulation results

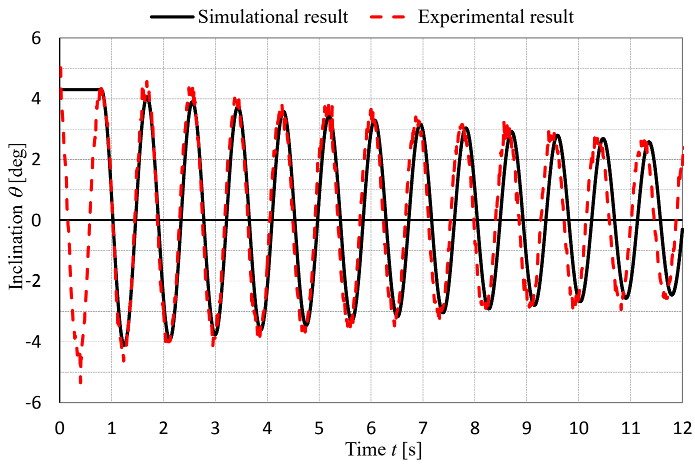

Fig. 9 Simulation and experiment result

Figure 8 shows two responses of the inclination angle in the cases, ρ_z=0, $\rho_{\theta ALL}$=0 and ρz=18.97 [mN/(m/s)], $\rho_{\theta \mathrm{ALL}}$=0.332 [mN/(rad/s)]. The eddy current loss gives more stability to the single point suspended EMS. Next, authors made an experiment by using the actual carrier under the same initial condition as the simulation, to confirm the modeling validity of the rolling motion. Figure 9 shows the simulational and experimental responses of the inclination angle. The experimental result seems to include an initial disturbance due to handling at the start. So, simulation started from the first peak of the experimental response.

In Figure 9, the simulation result confirmed validity of evaluation of dumping effect due to eddy current loss. However, there is a periodic deviation between simulational and experimental responses. The causes of this are erastic forces of the feed and signal lines from the ground side, calculation errors for the attractive force, the torque, and the moment of inertia of the carrier.

6. Conclusion

We derived damping factors of the rolling motion of the single point suspended EMS carrier, then constructed the model of the rolling motion, following the modeling of pitching motion. This paper confirmed validity evaluation of damping factor by eddy current loss. A period of the rolling motion needs more consideration. We are planning to make a new single point suspended EMS, which takes more advantage of damping effect due to eddy current loss.

References

[1] T. Takahashi, J. Okubo and M. Morishita: A Study on The Maglev Model of One Point Support Magnetic Suspension System.LD,43-48,(2011)

[2] Y. Nakamura and M. Morishita: Investigation of Eddy Current Swing Damping for Electro Magnetic Suspension

System, Journal of Applied Electromagnetics and Mechanics 50 (2015) 1–4
[3] M. Morishita and T. Azukizawa: ”Zero Power” Control Method for Electromagnetic Levitation System, IEEJ, IAS, 108(5), 447-454, (1988)
[4] T. Takahashi and M. Morishita: A Study on Propelling Coils for a Carrier System with The Single Point Suspended EMS, IEEJ, LD-13-105, (2013)